

## §14. Radial Electric Field Control by Electrode Biasing in LHD

Kitajima, S., Sasao, M., Okamoto, A., Ishii, K., Sato, Y., Kanno, M., Tachibana, J., Koike, S. (Dept. Eng. Tohoku Univ.), Inagaki, S. (RIAM, Kyushu Univ.), Takayama, M. (Akita Prefectural Univ.), Takahashi, H., Masuzaki, S., Shoji, M., Ashikawa, N., Tokitani, M., Yokoyama, M., Suzuki, Y., Satake, S., Shimozuma, T., Ido, T., Shimizu, A., Nagayama, Y., Tokuzawa, T., Yoshimura, S., Nishimura, K., Morisaki, T., Kubo, S., Kasahara, H., Mutoh, T., Yamada, H.

The effects of the ion viscosity maximum on the transition to an improved confinement mode were experimentally investigated by the externally controlled  $\mathbf{J} \times \mathbf{B}$  driving force for a poloidal rotation using the hot cathode biasing in Tohoku University Heliac (TU-Heliac).<sup>1-2)</sup> Here,  $\mathbf{J}$  and  $\mathbf{B}$  are a biasing electrode current and a magnetic field. In steady state the  $\mathbf{J} \times \mathbf{B}$  driving force balances with the ion viscous damping force and the friction to neutral particles. Then the local maximum in ion viscosity can be evaluated experimentally from the external driving force at the transition (critical driving force). The remaining problems in the biasing experiments on TU-Heliac were (1) to spread a ripple component in magnetic configuration to a lower region, and (2) to improve a target plasma to a high-performance region. In LHD the effective helical ripple  $e_{\text{eff}}$  and viscosity maxima have wider region than those in TU-Heliac. In this contribution we report on the difference of the transition condition in three configurations by the electrode biasing experiments in LHD.

The target plasma for the biasing in LHD was produced by ECH ( $f = 77$  and  $84$  GHz,  $0.2 < P_{\text{ECH}} < 0.5$  MW) in magnetic configurations ( $R_{\text{ax}} = 3.53, 3.60$  and  $3.75$  m,  $1.5 < B_t < 2.75$  T). The electron density and temperature at the magnetic axis were  $1 \sim 9 \times 10^{18} \text{ m}^{-3}$  and  $\sim 0.8$  keV in the Helium target plasma. The electrode was a cylindrical disk of diameter 100 mm and length 40 mm, made of Carbon and inserted to  $\rho_E \sim 0.8$ .

We compared the external driving force  $\mathbf{J} \times \mathbf{B}$  required for the improved mode transition in 3 configurations ( $R_{\text{ax}} = 3.53, 3.60$  and  $3.75$ ). Figure 1(a) shows the configuration dependence of the critical driving forces, which were evaluated at the forward and backward transition point. Figure 1(a) also shows the viscosity maximum  $\Pi_{p,n,LM}$  predicted by the neoclassical theory.<sup>3)</sup> The viscosity maximum increases according to the increase in  $R_{\text{ax}}$ . In the  $R_{\text{ax}} = 3.75$  case we cannot observe the transition, because the required electrode voltage exceed the limitation of the power supply. The critical driving force and the viscosity maximum have the same tendency including the result in the  $R_{\text{ax}} = 3.75$  case. Critical driving forces at the backward transition were smaller than that at the forward transition, which means the improved mode can be sustained by the smaller driving force in the backward transition phase and is consistent with transition scenario caused by the local

maximum in the ion viscosity. We also compared the configuration dependence of radial resistivity in L-mode with the theory. In Fig. 1(b)  $dM_p/dI_{p,n}$  was calculated from the viscosity in the low Mach number region. This value is proportional to  $dV_E/(dI_E/n_e)$  evaluated from the electrode characteristics. And these two values represent the radial resistivity. From Fig. 1(b) it is clear that two parameters in L-mode decrease with  $R_{\text{ax}}$  going outward.

Furthermore we measured space potential profiles by HIBP under the electrode biasing as shown in Fig. 2. The radial potential shifted to a positive direction keeping a broad profile according to the increase in the electrode voltage, which suggests the increase in the radial electric field in the plasma periphery that was the outside of the HIBP observation area.

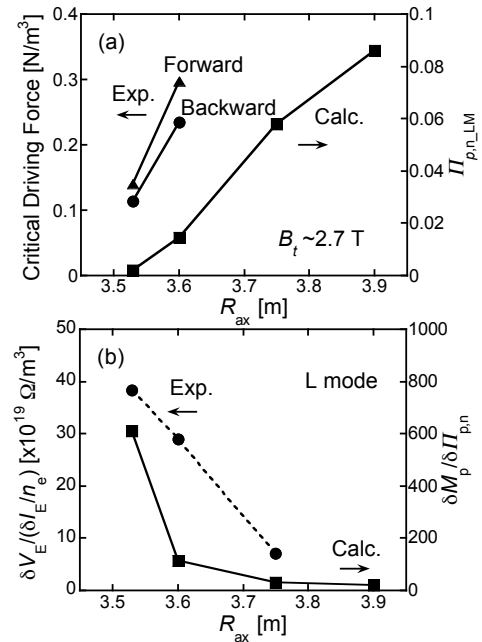


Fig. 1 Relation between (a) the critical driving force and the magnetic axis position, (b) the radial resistivity and the magnetic axis position

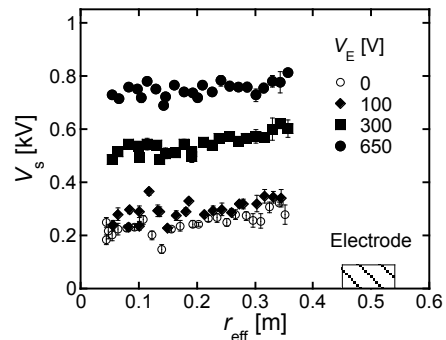


Fig. 2 Space potential profiles measure by HIBP

- 1) H. Takahashi *et al.*, *Plasma Phys. Control. Fusion*, **48**, 39 (2006).
- 2) S. Kitajima *et al.*, *Nucl. Fusion*, **46**, 200 (2006).
- 3) K. C. Shaing: *Phys. Rev. Lett.* **76**, 4364 (1996).